Time-domain surface profile imaging via a hyperspectral Fourier transform spectrometer

Julia Rentz Dupuis* and M. Selim Ünlü

Department of Electrical and Computer Engineering, Boston University, 8 Saint Mary's Street, Boston, Massachusetts 02215, USA

**Corresponding author: jrentz@optra.com*

Received April 8, 2008; accepted April 28, 2008;
posted May 7, 2008 (Doc. ID 94722); published June 13, 2008

We describe a method for time-domain surface profile measurements via white-light reflection spectroscopy using a hyperspectral Fourier transform spectrometer (HS-FTS). This technique measures the frequency of the spectral modulation of reflected light from a multilayer optical surface and reports the spatially resolved optical thickness. Owing to the Fourier relationship, the Fourier transform spectrometer manifests this spectral modulation as temporal satellites in interferogram space. We show that measurement of the positions of these satellites can be used to reconstruct the optical thickness profile over a surface using the HS-FTS. © 2008 Optical Society of America

OCIS codes: 240.0310, 110.4234, 120.2830.

The development of a hyperspectral Fourier transform spectrometer (HS-FTS) for surface profile imaging with a primary application of biological binding measurements has been previously reported [1]. This instrument was designed to operate in two modes: white-light reflection spectroscopy (WLRS) and spectral self-interference fluorescence microscopy (SSFM); however, the demonstration reported in this Letter was done using the WLRS mode alone. The measurement exploits the spectral content of the light reflected from a multilayer surface to decipher the optical thickness of a biomolecular layer bound to the surface. WLRS can therefore be used to measure changes in mass per unit area at the surface caused by a biological binding event. More generally, WLRS can be used as an all-purpose thin-film surface profiler.

The application of the HS-FTS to this measurement allows for spatially resolved optical thickness determination of a surface thereby enabling high throughput measurements. As for the previous reporting, the optical thickness determinations were made in spectral space, meaning an interferogram cube was collected and Fourier transformed, and each spatially resolved spectrum was fit to a curve in a least-squares sense to extract the desired optical thickness information. While the data reduction worked well, the time required to acquire the interferogram cube and process the data limited the system to nondynamic applications. In this Letter we present a new data reduction technique performed in the time domain. The new technique exploits the fact that a frequency shift in the spectral domain, which is the quantity of interest for both WLRS and SSFM measurements, exhibits itself as a shift in the location of temporal satellites in the time domain. Here we present concepts for measuring the locations of these satellites and correlating the locations with optical thickness using WLRS to demonstrate the concept. Unlike white-light interferometric techniques [2,3], ours does not require the sample to be aligned inside the interferometer. While a comparable approach employing FTS has been demonstrated [4], our work features two key differences: the imaging capability using a 2D focal plane array and the use of envelope detection of the satellites' positions rather than traditional peak detection. The latter feature allows us to work over narrower spectral ranges such as a fluorescence emission spectrum, which results in broad satellites that cannot be easily located via simple peak detection.

The WLRS concept has been described in detail in the literature [1,5,6]. Briefly, if we consider a silicon (Si) substrate with a thin layer (5 to 10 μm) of silicon dioxide (SiO_2) thermally grown on it, with WLRS, incident broadband light reflected by the substrate exhibits a sinusoidal spectral structure owing to the thin-film interference between the wave reflected by the air–SiO_2 interface and the wave reflected by the SiO_2–Si interface. The frequency of the spectral modulation is proportional to the optical thickness of the SiO_2 layer *plus* any feature such as biomolecular material bound to it. The WLRS interference equation can be approximated by

$$I(\sigma) = I_2 + I_3 + 2\sqrt{I_2 I_3}\cos[4\pi n_2 \sigma(t + \delta t)], \qquad (1)$$

where σ is the optical frequency (in units of cm^{-1}); I_2 and I_3 are the intensities reflected at the air–SiO_2 and SiO_2–Si interfaces, respectively; n_2 is the refractive index of SiO_2; t is the SiO_2 physical thickness; and δt is the height of the feature. For the biological measurements it is sufficient to assume the refractive index of the biological material is approximately equal to that of the SiO_2 (1.45) [7]. Although Eq. (1) neglects multiple reflections, it is sufficiently accurate for spectral fitting purposes.

If we take Eq. (1) as the Fourier or frequency domain expression of the thin-film interference, the time-domain expression, which is effectively what the Fourier transform spectrometer (FTS) physically measures, is the inverse Fourier transform of Eq. (1):

$$IFT[I(\sigma)] \propto I_2 + I_3 + \sqrt{I_2 I_3}(\delta\{B(\tau) - [2n_2(t+\delta t)]\} + \delta\{B(\tau) + [2n_2(t+\delta t)]\}), \quad (2)$$

where $B(\tau)$ is optical retardation as a function of time. Equation (2) is an expression of the temporal satellites we see in the interferogram whose positions relative to the zero optical path difference (or to each other) are proportional to the optical thickness of the SiO_2 layer plus the feature. These satellites appear as reduced amplitude copies of the centerburst whose shape is dictated by the spectral range of the instrument. Figure 1 shows interferograms acquired from 5 and 10 μm SiO_2 samples using our experimental setup; these data clearly show that the satellites of the centerburst increase in separation by a factor of 2 between 5 and 10 μm SiO_2. Note that the actual centerburst itself is not used in the calculations and was intentionally saturated to increase the signal-to-noise ratio of the satellites.

For this proof of principle, we calculated the satellite separation using three different methods. The first method was to subtract the mean from the interferogram, rectify the result, calculate the center of mass of each satellite, and take the difference between them. The second method was to subtract the mean, rectify, determine the envelope of each satellite by identifying the peaks, interpolate the envelopes to a fixed number of points, calculate the center of mass of the envelopes, and take the difference between them. The final method was to subtract the mean, rectify, determine the envelope of each satellite, interpolate the envelopes, fit the envelopes to a Gaussian function in a least square sense, and subtract the means of the two Gaussian fits. Transfer functions converting satellite shift to height information were determined analytically. These calculations were performed on a per pixel basis thereby reducing the three-dimensional interferogram cube to a two-dimensional height image. All calculations were done in MATLAB.

Figure 2 shows the configuration of the HS-FTS used for this WLRS measurement. The spectral range of the light detected by the CCD was estimated through a combination of the spectral operating properties of the beam splitters, lenses, and the CCD and

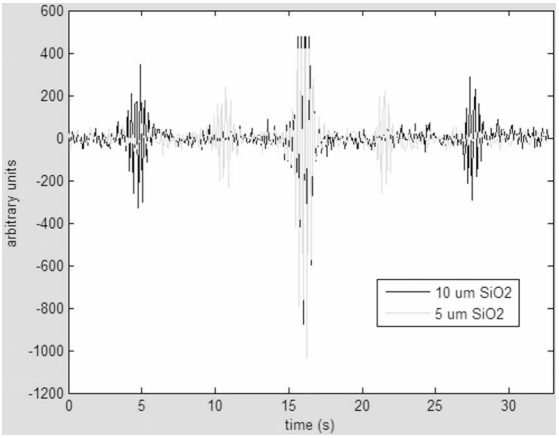

Fig. 1. Measured temporal satellites.

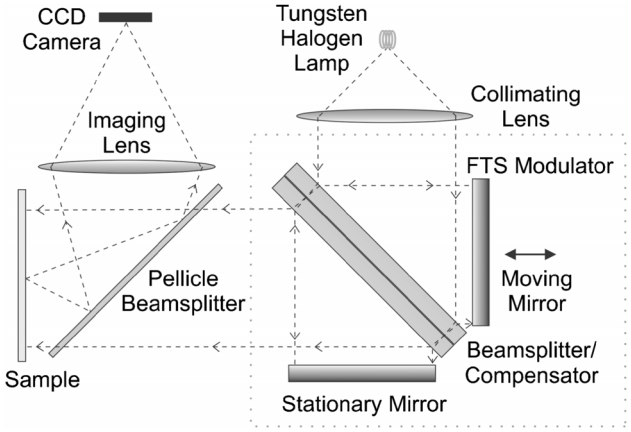

Fig. 2. HS-FTS configuration for WLRS measurement.

also by the width of the centerburst and satellites. The estimated range based on these factors was approximately 600 to 800 nm. For these measurements we scanned the interferometer mirror over an optical retardation range of ±40 μm in 400 steps of 200 nm each. These parameters support the required scan range to acquire the satellites for 10 μm SiO_2 with sufficient point density. A single scan is acquired in approximately 32 s. However, for future applications it is actually not necessary to scan the entire range; since the interferometer has absolute mirror position feedback provided by the laser reference [1], the mirror can simply be scanned back and forth over a single satellite that covers approximately 25 samples. A single optical thickness measurement can therefore be made in 2 s. Further improvements to the interferometer servo will decrease this time further.

Measurements were made of a positive photolithographically etched 10 μm SiO_2 artificial sample with approximately 40 nm deep etched features. Ten scans were acquired, and the satellite portions were isolated as 25 point arrays. Height images were then calculated via the three methods previously described. We also calculated the per scan noise equivalent vertical displacement, or NEΔZ, for each method by taking the standard deviation of the difference between two height images, each calculated from a single scan, and dividing by the square root of 2 to account for the two independent noise sources. The sample's feature depths were verified using a commercially available white-light interferometer system.

Figure 3 shows reconstructed height images using the three methods described. Grayscale units are in nanometers with an assumed refractive index of 1.45. With each height image is a crosscut taken over row 91. As can be seen in both the height image and the crosscut, reconstruction by method 1 results in an effect at the edges of the features. We see that this effect becomes much less in the two envelope reconstructions (methods 2 and 3); we therefore attribute the edge effect primarily to the weighting of nonpeak points in the satellites to the center of mass calculation near the edges. Calculating the envelopes of the satellites removes the nonpeak points and minimizes

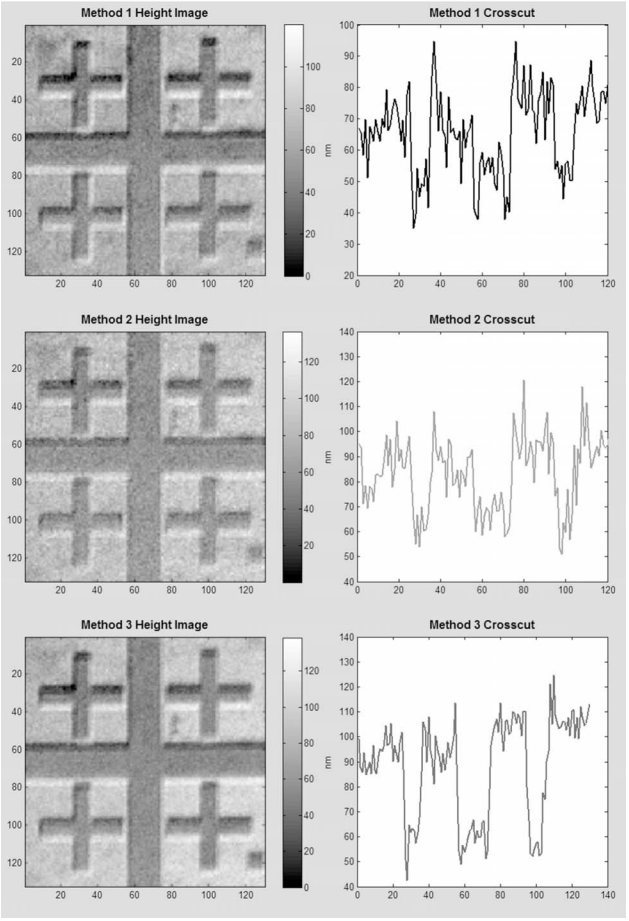

Fig. 3. Reconstructed height images and crosscuts.

the edge effects. Reconstruction method 2 appears to produce a more accurate image than method 1; however, it also appears noisier than method 1 most likely because of the dropped data points. Reconstruction method 3 shows the most accurate image and appears to have a noise level comparable to method 1.

The per scan NEΔZ calculations were as follows: 15.2 nm for method 1, 20.8 nm for method 2, and 16.6 nm for method 3. We would expect the NEΔZ for method 2 to be worse than method 1 since data points were dropped; we would also expect the NEΔZ for method 3 relative to method 2 to improve owing to the curve fitting. With respect to computation time, method 1 is by far the fastest (on the order of a few seconds for the 130×130 height image), as it is effectively straight algebra with no curve fitting. Method 2 requires on the order of 1 min for the extra logic to identify the peaks of each satellite. Method 3 requires on the order of a few minutes for the envelope detection and additional Gaussian fitting. Note that use of a single satellite is expected to increase the NEΔZ in each case by a factor of $\sqrt{2}$.

In summary, we demonstrated the proof of principle of time-domain optical thickness–height calculations using the HS-FTS. We described an approach for correlating the positions of temporal satellites relative to each other with optical thickness by their Fourier relationship using WLRS. We demonstrated this technique on a positive photolithographically etched 10 μm SiO_2 artificial sample and showed three different reconstruction methods. The first method, involving a center of mass calculation on each satellite, proved to be the fastest and had the lowest noise but also exhibited artifacts at the edges of the features. The third method, based on a Gaussian fitting of the satellite envelopes, shows the most accurate reconstruction with comparable noise performance to the first method; however, the computation time was much longer. Overall, we believe this to be a viable surface profiling technique that can acquire the relevant data in 2 s with the current hardware system. Future improvements to the interferometer's servo should decrease the acquisition time further.

This approach can be extended to the SSFM measurement where the spectral range will be decreased to approximately 100 nm because of the fluorescence emission spectrum. In this case the satellites will be effectively twice as wide, owing to the Fourier relationship. The effect on the resolution and accuracy of the measurement will need to be determined.

This work was supported by the National Science Foundation, grant R21 GM074872-01A1. The Fourier transform spectrometer was developed by Optra, Inc., of Topsfield, Massachusetts.

References

1. J. R. Dupuis, J. Needham, E. Özkumur, D. A. Bergstein, B. Goldberg, J. R. Engel, D. L. Carlson, and M. S. Ünlü, Appl. Opt. **47**, 1223 (2008).
2. M. Hart, D. G. Vass, and M. L. Begbie, Appl. Opt. **37**, 1764 (1998).
3. A. Harasaki and J. C. Wyant, Appl. Opt. **39**, 2101 (2000).
4. Z. Zhou and R. Reif, IEEE Trans. Semicond. Manuf. **8**, 333 (1995).
5. L. Moiseev, M. S. Ünlü, A. K. Swan, B. B. Goldberg, and C. Cantor, Proc. Natl. Acad. Sci. USA **103**, 2623 (2006).
6. M. S. Ünlü, I. E. Özkumur, D. A. Bergstein, A. Yalcin, M. F. Ruane, and B. B. Goldberg, in *Biophotonics: Biological and Medical Physics, Biomedical Engineering*, L. Pavesi and P. M. Fauchet, eds. (Springer, in press).
7. S. Elhadj, G. Singh, and R. F. Saraf, Langmuir **20**, 5539 (2004).